A Cycloaddition Model for Fullerene Formation

2 AUTHORS, INCLUDING:

Douglas L. Strout
Alabama State University

54 PUBLICATIONS   **1,393** CITATIONS

SEE PROFILE

A Cycloaddition Model for Fullerene Formation

Douglas L. Strout and Gustavo E. Scuseria*

Center for Nanoscale Science and Technology, Department of Chemistry and Rice Quantum Institute, Rice University, MS 60, Houston, Texas 77005-1892

Received: October 11, 1995[⊗]

Since their discovery, the fullerenes have challenged scientists with a wide array of problems concerning their properties, behavior, and potential applications. One such fundamental question is that of the assembly of these carbon cages. Much effort has been directed at obtaining an understanding of the process whereby graphite is transformed into fullerenes. In a previous work, we introduced a novel interpretation of the ion chromatography results from fullerene generation experiments. In this work, that interpretation is expanded and ab initio calculations are performed to illustrate how the model explains the experimental results. This "cycloaddition model" is then used to develop a plausible fullerene assembly mechanism.

Introduction

In 1985, the discovery[1] of buckminsterfullerene (BF) prompted a flurry of activity as scientists sought to characterize this new form of carbon and produce it in bulk quantities. When bulk synthesis[2] was achieved in 1990, scientific investigation of buckminsterfullerene intensified and diversified as various research groups produced a wide array of both endohedral and exohedral derivatives. A fundamental question about C_{60} and the other fullerenes is the mechanism of their formation. What happens to graphite after it is vaporized which leads to the appearance of carbon cages?

A range of experiments have been conducted to elucidate the formation of fullerenes. Ebbesen *et al.*[3] generated fullerenes by the resistive heating of two graphite rods with different abundances of carbon-13. The purpose of the experiments was to determine the form in which graphite is removed from the surface of the rods. For example, if graphite were removed from the rods in sections large enough to close and form C_{60} independently, the mass spectrum of the C_{60} products should show two distinct mass distributions corresponding to the isotope ratios of the two rods. However, this was not observed. The C_{60} products showed mass distributions that indicated thorough isotopic mixing. This demonstrated that graphite is converted to an atomic carbon vapor before fullerenes are formed.

In another experiment, McElvany *et al.*[4] generated fullerenes from carbon rings produced by the laser desorption of organic precursors. C_{18}, C_{24}, and C_{30} were each used in a separate experiment. In each case, the mass spectra of the products showed peaks at integer multiples of the mass of the initial carbon ring. The C_{30} experiment showed an enormous peak at C_{60} and much smaller peaks at C_{90}, C_{120}, etc. C_{18} and C_{24} both produced large C_{70} peaks, because both can form C_{72}, which then dissociates C_2 to give the stable C_{70}. These experiments demonstrated that carbon rings can be converted to fullerenes, but does a rings-to-fullerenes assembly pathway have any application when graphite is the starting material?

Recently, a powerful tool has been introduced for examining the details of graphite vaporization experiments. An experimental technique, known as "ion chromatography",[5] has revealed new insights into the fullerene formation experiments. With this technique, the cluster ions produced by graphite vaporization are mass-selected and injected into a tube that is filled with an inert gas, usually helium. Collisions between the clusters and the inert gas cause the clusters to be separated by cross section, as the more compact clusters exit the tube at earlier times. The resulting plot of cluster intensity vs time is called an "arrival time distribution" (or ATD).

von Helden *et al.*[6] performed ion chromatography on the graphite vaporization products and reported several peaks in the ATD. For carbon clusters with 10–20 atoms, a single peak appeared. Beginning with C_{21}, two peaks were observed, and for 30 or more atoms, three more peaks were seen, for a total of five. Those authors also developed a method for assigning the arrival time peaks to structural cluster isomers. For each proposed structural isomer, they optimized the geometry using the semiempirical PM3 method. Each optimized geometry was then used for a Monte Carlo simulation of the collisions between the proposed cluster and the helium atoms. This procedure yields a theoretical cross section for the cluster, which is then converted to a convenient scale called the "mobility" scale. The experimental arrival times are also converted to mobilities, and if a match is obtained, the proposed cluster is assigned to the experimental peak.

According to the von Helden *et al.* model,[6] the peak that is seen beginning at C_{10} corresponds to a monocyclic carbon ring and is called the "ring I" peak. The second peak observed at C_{21} is denoted the "ring II" peak and assigned to planar bicyclic rings. One of the three peaks appearing at C_{30} is named "ring III" and is interpreted as planar tricyclic structures. Another peak is of very low intensity and has been dubbed "3-D ring". The interpretation of the 3-D ring peak was not clearly made, although graphitic sheets were suggested as a possibility. The final peak, corresponding to the most compact structures observed in the experiment, is assigned to fullerenes.

Following the method of von Helden *et al.*,[6] Book *et al.*[7] developed a mobility code and demonstrated two essential points about the theoretical mobilities. First, theoretical mobilities were shown to be insensitive to molecular vibration. This validates the use of static, equilibrium geometries for the mobility calculations. Also, these mobilities were shown to be insensitive to the choice of the level of theory employed when obtaining optimized geometries. Therefore, fast, semiempirical methods can be used to obtain valid geometries quickly.

Recently, we proposed an alternative interpretation[8] of the ion chromatography experiments. The model is based on cycloaddition reactions between monocyclic carbon rings. Using a semiempirical tight-binding (TB) carbon–carbon

A Cycloaddition Model for Fullerene Formation

J. Phys. Chem., Vol. 100, No. 16, 1996 **6493**
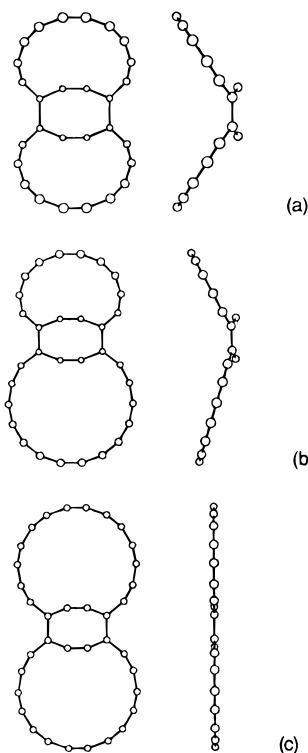
Figure 1. Two perpendicular views of 4 + 4 cycloadducts: (a) C_{28}, (b) C_{32}, and (c) C_{36}.
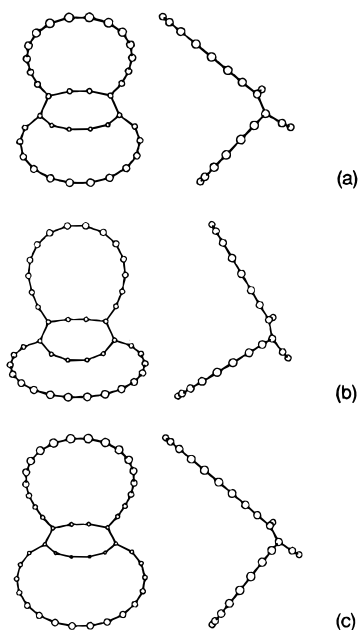
Figure 2. Two perpendicular views of 4 + 6 cycloadducts: (a) C_{36}, (b) C_{40}, and (c) C_{44}.

potential[9] to optimize geometries and the Book *et al.* mobility code, we demonstrated that 2 + 2 cycloadducts have ring II mobilities and that 2 + 4 cycloadducts have ring III mobilities. In the present work, we generalize this "cycloaddition model" by investigating 4 + 4 and 4 + 6 cycloadducts, which are pictured in Figures 1 and 2, respectively. Mobility results for the 4 + 4 cycloadducts, shown in Table 1, demonstrate that 4 + 4 adducts are not a good match for ring II except at large cluster sizes and therefore not a probable source of ring II clusters. The 4 + 6 mobilities in Table 2 show that these adducts match ring III mobilities just as well as 2 + 4 adducts, thereby demonstrating the existence of two families of cycloadducts that are good candidates for ring III clusters.

TABLE 1: Mobilities of 4 + 4 Cycloadducts Compared to Ring II Results and 2 + 2 Cycloadducts (Mobilities in cm²/V s)

cluster size	ring II	adduct	4 + 4	2 + 2
C_{28}		14 + 14	4.70	4.24
C_{32}		14 + 18	4.01	3.69
C_{36}	3.30	18 + 18	3.47	3.29
C_{40}	2.92	22 + 18	3.04	2.92
C_{44}	2.7	22 + 22	2.76	2.64
C_{48}	2.45	26 + 22	2.47	2.40

TABLE 2: Mobilities of 4 + 6 Cycloadducts Compared to Ring III Results and 2 + 4 Cycloadducts (Mobilities in cm²/V s)

cluster size	ring III	adduct[a]	4 + 6	2 + 4
C_{36}	3.70	18 + 18	3.75	3.64
C_{40}	3.26	22 + 18	3.31	3.23
C_{44}	2.95	22 + 22	2.97	2.87
C_{48}	2.7	26 + 22	2.65	2.71

[a] For asymmetric additions, the ring listed first contributes the larger number of atoms to the cycloaddition.

However, no interpretation of the ion chromatography experiments can stand on mobility results alone. Theoretical mobilities only show that a given cluster is consistent with an experimental observation, and a match between theoretical and experimental mobilities does not constitute proof that the candidate is, in fact, the observed cluster. In the present work, high-level ab initio calculations are used to provide further support to the cycloaddition model. Also, since these cycloadducts are produced in the same experiments which produce fullerenes, a model will be developed for the formation of fullerenes from the cycloadducts.

The Case for 2 + 4 and 4 + 6 Cycloadducts

The mobility results establish the cycloadducts as possibilities for the clusters generated by graphite vaporization, but other questions remain. Why do 2 + 2 cycloadducts appear for cluster sizes throughout the twenties, whereas 2 + 4 cycloadducts are not seen until C_{30}? The question of whether or not a given cluster appears involves the energetics of the reaction that produces it. Detailed, accurate energies of reactants, products, and transition states are needed, and for that high-level ab initio calculations are required. Geometries for the monocyclic rings, cycloadducts, and transition structures are optimized with the Hartree−Fock (HF) method using a double ζ (DZ), or 4s2p, basis set formed by contracting the Huzinaga−Dunning[10] (9s5p) uncontracted Gaussian basis.

Energies at the DZ HF geometries are computed with density functional theory (DFT) using a double ζ plus polarization (DZP) basis, consisting of the DZ basis plus polarization function $\alpha_d = 0.75$. The particular DFT method in this work employs the nonlocal (gradient-corrected) Becke[11] exchange functional and the nonlocal Perdew[12] correlation functional. This Becke−Perdew method is denoted BP. Hartree−Fock calculations are carried out by using the TURBOMOLE quantum chemistry package,[13] and DFT is introduced through a separate code[14] which interfaces with TURBOMOLE.

Density functional theory is implemented as a hybrid with Hartree−Fock, meaning that the exchange and correlation energies are computed using the Hartree−Fock electron density rather than a DFT density. The DFT total energies are computed by subtracting the HF exchange from the HF total energy and adding the DFT exchange and correlation energies. That is,

$$E^{\text{DFT}} = E^{\text{HF}} - E_x^{\text{HF}} + E_x^{\text{DFT}} + E_c^{\text{DFT}}$$
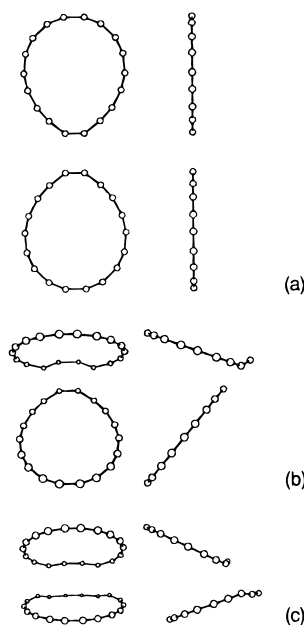
Figure 3. C_{36} transition states for $C_{18} + C_{18}$ cycloaddition: (a) $2 + 2$, (b) $2 + 4$, and (c) $4 + 6$.

TABLE 3: DZP BP Barriers to Cycloaddition Processes (Barriers in eV)

process	C_{20} 10 + 10	C_{24} 10 + 14	C_{28} 14 + 14	C_{32} 14 + 18	C_{36} 18 + 18
2 + 2	2.38	2.66	2.06	2.69	1.91
2 + 4	1.61	1.27	1.05	0.90	0.93
4 + 6		1.80	1.38	1.33	0.91

for a general density functional method, where E_x and E_c represent exchange and correlation energies, respectively.

The particular clusters studied include monocyclic rings C_{10}, C_{14}, and C_{18}. These rings are chosen because they are Hückel $4n + 2$ rings. Cycloadducts with 20−36 atoms are selected because this range of sizes includes clusters on both sides of the appearance threshold for ring III and should allow for a thorough exploration of the cycloaddition processes. The DZP BP method is employed to explore $2 + 2$, $2 + 4$, and $4 + 6$ cycloaddition. Energies for $2 + 4$ and $4 + 6$ cycloadducts are computed for the singlet ground states, and $2 + 4$ and $4 + 6$ transition states are also optimized as singlets. Transition states for $2 + 2$ cycloaddition have triplet electronic configurations as indicated by the Woodward−Hoffmann rules. The $2 + 2$ adducts themselves are predicted by DZ HF to have triplet ground states. However, DZP BP predicts singlet states for the $2 + 2$ adducts, so the results reported in this work are for singlet $2 + 2$ cycloadducts.

The first question to be answered by these calculations is whether the transition barriers for $2 + 2$, $2 + 4$, and $4 + 6$ cycloaddition are a function of cluster size over the range of 20−36 atoms. Transition states for several cycloadditions are shown in Figure 3. If the barriers to $2 + 4$ and $4 + 6$ are appreciably higher for sizes below C_{30} than above C_{30}, then the appearance threshold for ring III can be explained simply as a result of prohibitively high reaction barriers below the threshold. DZP BP barriers are shown in Table 3 and do not show the large changes in energy required to explain the appearance thresholds. The $2 + 2$ barriers are within a few tenths of an electronvolt of each other over the range of 20−36 atoms, which is consistent with experiment because $2 + 2$ adducts are observed throughout the size regime considered. However, $2 + 4$ and $4 + 6$ barriers across the C_{30} threshold also do not vary by more than a few tenths of an electronvolt.

TABLE 4: DZP BP ΔE for Cycloaddition Processes (Energies in eV)

process	C_{20} 10 + 10	C_{24} 10 + 14	C_{28} 14 + 14	C_{32} 14 + 18	C_{36} 18 + 18
2 + 2	−2.35	−2.46	−2.51	−2.46	−2.42
2 + 4	−0.24	−1.26	−1.73	−2.10	−2.20
4 + 6	−0.59	−1.29	−1.81	−2.21	−2.25

These barriers do not provide any explanation why $2 + 4$ and $4 + 6$ cycloadducts should form selectively at sizes above C_{30}.

However, under the Woodward−Hoffmann rules for cycloaddition processes, the symmetry rules that permit a cycloaddition to occur also permit the reverse process. A cycloaddition may occur and be immediately followed by the corresponding retrocycloaddition. This makes it important to determine ΔE for the cycloaddition processes because the reverse barrier equals the forward barrier minus ΔE. The DZP BP ΔE data for the cycloadducts are shown in Table 4, and these data provide a clear explanation for the observed appearance thresholds. The $2 + 2$ cycloadditions are exothermic by more than 2 eV (nearly 50 kcal/mol) over the entire range from 20 to 36 atoms. Once formed, a $2 + 2$ cycloadduct would be stable enough to resist dissociation back to its constituent carbon rings. For larger clusters, such as C_{32} and C_{36}, the $2 + 4$ and $4 + 6$ cycloadducts have stability similar to the $2 + 2$ adducts. However, for the smaller clusters, the $2 + 4$ and $4 + 6$ cycloadducts are much less stable and may dissociate back to their original monocyclic rings. This is the explanation that demonstrates that $2 + 4$ and $4 + 6$ cycloaddition are consistent with experimental observations about ring III. The $2 + 4$ and $4 + 6$ cycloadducts are formed at all cluster sizes above 20 atoms but are only observed (as ring III) above 30 atoms because the smaller ones return to their reactants.

If resistance to retrocycloaddition is the key to whether a given cycloadduct will be experimentally observed, then the DZP BP level of theory can be used to establish an empirical rule that a cycloaddition process that is exothermic by more than 2 eV will produce an adduct that resists dissociation. This rule would predict $2 + 2$ adducts at all sizes from 20 to 36 atoms and $2 + 4$ and $4 + 6$ adducts at sizes with more than 30 atoms, which is consistent with the experimental observations. This rule is qualitative in nature and only applies to the DZP BP level of theory, and there certainly exists no physical reason why 2 eV should be the threshold. Higher levels of theory, such as coupled-cluster theory (as CCSD or CCSD(T)), could reflect the same behavioral trends as DZP BP and show a different threshold. This "2 eV rule" is simply a guideline for evaluating the DZP BP results in this work.

The cycloaddition model, therefore, is consistent with two important experimental observations. First, the cycloadducts have been shown to have cluster mobilities that match the mobilities observed in the ion chromatography experiments. Also, the energetics of the cycloaddition reactions provide a clear and simple explanation for the observed cluster appearance thresholds.

The Fate of the Cycloadducts

What happens to the cycloadducts after they are formed? It has been suggested previously[15] that $2 + 2$ cycloadducts can transform to fullerenes, but this seems unlikely because $2 + 2$ adducts with 20−30 carbon atoms fail to produce fullerenes despite strong theoretical evidence[16] that fullerenes are much more stable than carbon rings that are seen in this size range. However, a $2 + 2$ cycloadduct can undergo a $2 + 2$ retrocycloaddition process which breaks two bonds to form a single
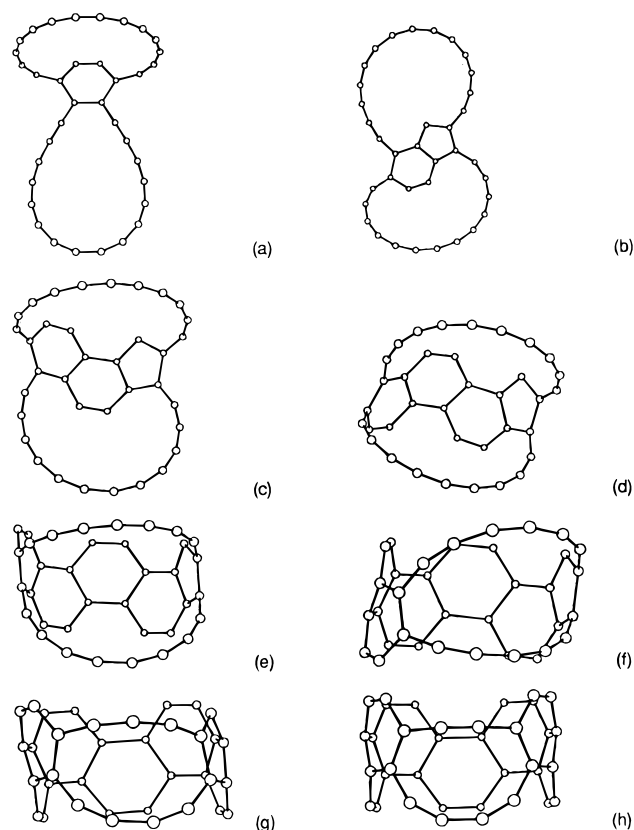
A Cycloaddition Model for Fullerene Formation

J. Phys. Chem., Vol. 100, No. 16, 1996 **6495**

Figure 4. Minima along the path from $C_{18} + C_{18}$ 2 + 4 cycloadduct to C_{36} hoop.

TABLE 5: TB Energetics of Pathway from 2 + 4 Cycloadduct to C_{36} Hoop as Shown in Figure 4 (Relative Energies in eV)

step	E (minima)	barrier (eV)
(a, adduct)	0.00	
		0.87
(b)	−0.29	
		1.16
(c)	−0.51	
		1.12
(d)	−0.85	
		1.01
(e)	−1.09	
		0.95
(f)	−1.47	
		1.00
(g)	−1.53	
		0.99
(h, hoop)	−2.66	

Figure 5. Minima along the path from $C_{18} + C_{18}$ 4 + 6 cycloadduct to C_{36} hoop.

TABLE 6: TB Energetics of Pathway from 4 + 6 Cycloadduct to C_{36} Hoop as Shown in Figure 5 (Relative Energies in eV)

step	E (minima)	barrier (eV)
(a, adduct)	0.00	
		0.90
(b)	−0.23	
		0.96
(c)	−0.56	
		1.03
(d)	−0.90	
		0.93
(e)	−1.18	
		0.97
(f)	−1.38	
		1.17
(g)	−0.86	
		0.64
(h, hoop)	−2.61	

large monocyclic ring. The newly formed large ring can react to form still larger cycloadducts. Larger 2 + 2 cycloadducts can react to form larger rings, and so on. Rings with as many as 60 atoms have been detected by ion chromatography techniques.[15]

The 2 + 4 and 4 + 6 cycloadducts have no such one-step, low-energy reaction that leads to a larger ring. However, these clusters can, with a modest barrier, undergo other reactions that lead instead toward carbon cages. In the present model, we present an example in which the cycloadduct undergoes a sequence of cyclizations that results in a cylindrical carbon species that is denoted here as a carbon "hoop". For a C_{36} 2 + 4 cycloadduct of two C_{18} carbon rings, the transformation to a hoop has been mapped out using the semiempirical TB method.[9] TB-optimized structures for the minima along the path are shown in Figure 4, and the TB energetics are presented in Table 5. At the TB level of theory, each step in the hoop formation
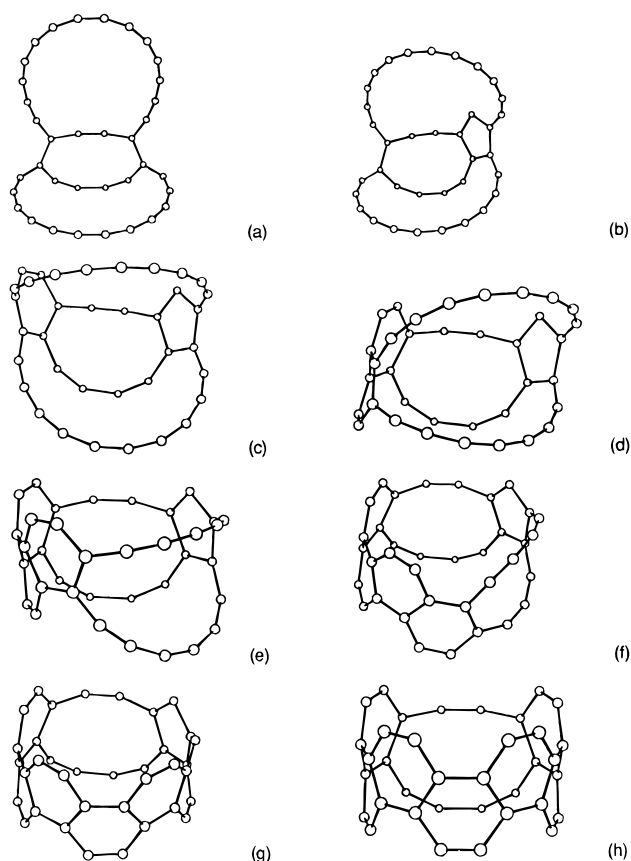
is exothermic and has a modest barrier. The overall process is exothermic by more than 2.5 eV. A similar hoop assembly exists for the C_{36} 4 + 6 cycloadduct. The minima are pictured in Figure 5, and detailed TB energetics are given in Table 6. The resultant hoop is identical to the one formed from the 2 + 4 adduct. Both cycloadducts are viable starting materials for hoop formation.

Do ab initio calculations also predict that hoops are stable? DZ HF optimizations have not been carried out at each step of hoop formation because of the expense of optimizing in C_1 symmetry (that is, no symmetry) and the difficulty of finding transition states in C_1 symmetry for large systems for which analytic energy second derivatives are computationally intractable. However, DZ HF optimizations have been performed on a sequence of the hoops themselves. Using these DZ HF geometries, DZP BP energies have been computed for hoops
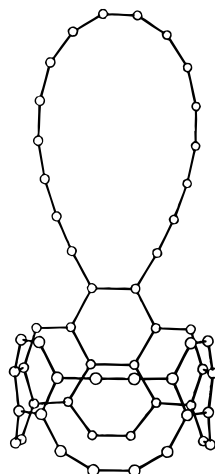
Figure 6. C_{54} 2 + 4 cycloadduct between C_{36} hoop and C_{18} monocyclic ring.

TABLE 7: DZP BP Energies of Carbon Hoops Relative to Monocyclic Precursors

hoop size	rings	E
C_{28}	14 + 14	−2.03
C_{32}	14 + 18	−2.45
C_{36}	18 + 18	−3.28
C_{40}	18 + 22	−3.80
C_{44}	22 + 22	−4.05
C_{48}	22 + 26	−4.21
C_{52}	26 + 26	−4.70
C_{56}	26 + 30	−5.24
C_{60}	30 + 30	−5.32

with 28 to 60 atoms. The DZP BP energetics are detailed in Table 7. This data illustrates that as cluster size increases, hoops become increasingly stable with respect to monocyclic precursors.

   The DZP BP energies at DZ HF geometries predict that the transformation from cycloadducts to hoops is energetically favorable for all cluster sizes for which the ring III species are observed experimentally. This mechanism also provides an explanation for the McElvany ring addition results[4] in which, for example, laser desorption of C_{18} rings results in a series of C_{18n} products. The hoop itself contains many sites suitable for further cycloaddition should it collide with another ring. Figure 6 illustrates an example, a 2 + 4 cycloadduct between a C_{18} ring and the C_{36} hoop. This adduct is a C_{54} object which could react with another ring, and so on, to form other cylindrical clusters. The pathway from cycloadducts to hoops introduces a significant amount of graphitic (sp^2) character which is evident in fullerenes. Hoop formation pathways are only an example of the ways in which cycloadducts can become more graphite like, and surely others exist as well. Can a hoop become a fullerene, which is an all-sp^2 molecule?

From Hoops to Cages

   Carbon hoops have a large number of triple bonds between atoms whose bond angles are far from 180°. The bond angle strain should make those sites very susceptible to reactions which rearrange the bonds. One such reaction is the 1,2-carbon shift. In a 1,2-carbon shift, a hexagon becomes a pentagon with a dangling atom attached, as illustrated in Figure 7. After two 1,2-shifts have occurred on neighboring triple bonds, the two dangling atoms can bond to each other to form a new pentagon or hexagon. In this way, a hoop can close its top and bottom faces with new polygons and thereby form a spherical cage.

   Energetics of 1,2-carbon shifts have been explored with the DZP BP method on DZ HF-optimized geometries. Calculations
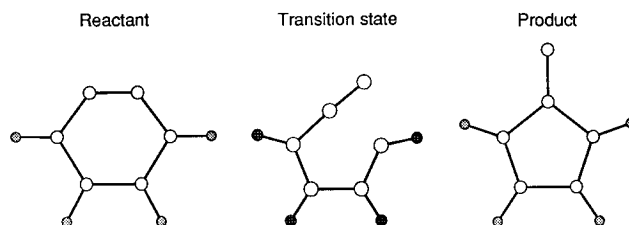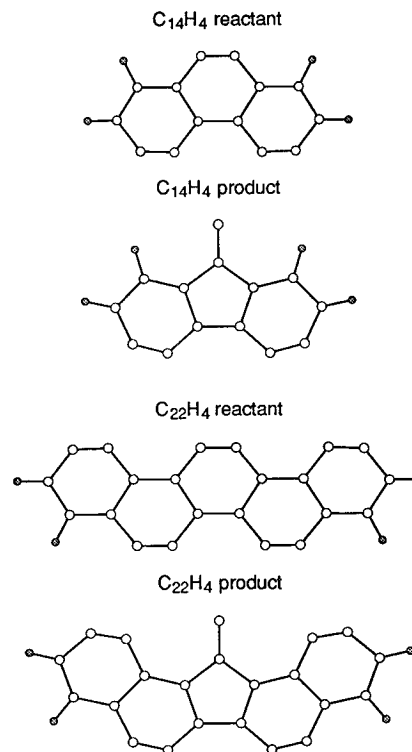

Figure 7. 1,2-Carbon shift.

$C_{14}H_4$ reactant

$C_{14}H_4$ product

$C_{22}H_4$ reactant

$C_{22}H_4$ product

Figure 8. 1,2-Carbon shifts on model systems.

TABLE 8: DZP BP Energetics of 1,2-Carbon Shifts (Energies in eV)

molecule	barrier	ΔE
$C_{14}H_4$	1.67	+1.15
$C_{22}H_4$	1.92	+1.28
C_{32} hoop		+1.91
C_{36} hoop		+1.33
C_{40} hoop		+1.69

are first performed on small model systems which simulate a section of a hoop, as shown in Figure 8. For these systems, which have hydrogen atoms replacing the connections to the rest of the hoop, minima and transition states have been optimized. The DZP BP energetics are presented in Table 8. For actual hoops, minima have been optimized for C_{32}, C_{36}, and C_{40}, and the energetics are also shown in Table 8. The DZP BP data indicate that the transition barriers for 1,2-shifts on the model systems are 1.67 and 1.92 eV. ΔE for small systems are between +1.1 and +1.3 eV. ΔE results for the carbon hoops qualitatively follow the data for the small molecules, and it is assumed that the transition barriers for the hoops similarly follow. The best results in this study indicate that a 1,2-shift occurs with a barrier of less than 2 eV.

   For the C_{36} hoop discussed in the previous section, the path from hoop to initial cage closure has been mapped using the semiempirical TB method. Minima and transition states are optimized, and the TB energetic data are shown in Table 9. Minima along the path are illustrated in Figure 9. The total process lowers the electronic energy of the cluster by 10.6 eV.
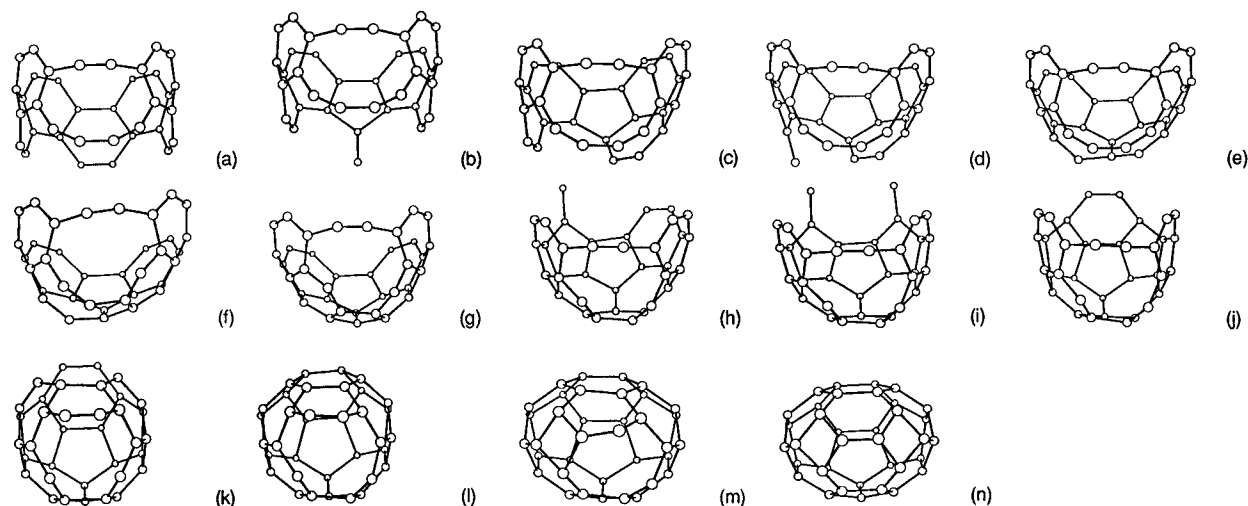
A Cycloaddition Model for Fullerene Formation

J. Phys. Chem., Vol. 100, No. 16, 1996 **6497**

Figure 9. Pathway from C_{36} hoop to a closed cage.

TABLE 9: TB Energetics for Pathway from C_{36} Hoop to a Closed Cage as Shown in Figure 8 (Energies in eV)

step	E (minima)	barrier (eV)
(a, hoop)	0.00	
		2.42
(b)	+1.21	
		2.62
(c)	−1.53	
		2.22
(d)	−0.56	
		0.00
(e)	−2.32	
		0.16
(f)	−4.12	
		0.00
(g)	−6.39	
		3.39
(h)	−4.14	
		3.22
(i)	−2.11	
		0.19
(j)	−5.77	
		2.18
(k)	−3.88	
		0.44
(l)	−9.54	
		0.66
(m)	−8.90	
		0.10
(n)	−10.57	

TABLE 10: DZP BP Energies of Fullerenes Relative to Monocyclic Precursors (Energies in eV)

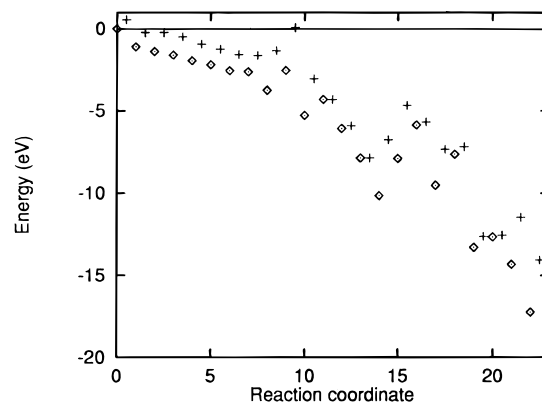| fullerene	rings	rel energy
C_{32}	14 + 18	−18.86
C_{36}	18 + 18	−21.86
C_{40}	18 + 22	−25.88
C_{44}	22 + 22	−30.29
⋮		
C_{60}	30 + 30	−50.13

Figure 10. TB energetics for a path from two C_{18} rings to the most stable C_{36} fullerene: minima are represented by diamonds; transition states, by crosses.

However, it is interesting to note that the initial cage closure does not yield the D_{2d} isomer which is known to be most stable. The cage must somehow find a way to its most stable form.

Annealing

Once the carbon cage is closed, it is not certain that the cage will be the most stable isomer for the particular fullerene. In fact, it is highly improbable that the fullerene generation experiments would yield the most stable isomer of any fullerene upon initial cage closure. However, the cages can isomerize by undergoing processes that rearrange the polygons composing the cage. Such reactions are collectively referred to as annealing processes. The best known annealing process is the Stone−Wales,[17] or pyracylene, rearrangement, in which a C_2 bond undergoes a 90° rotation such that two hexagons and two pentagons change places. The Stone−Wales reaction on the buckminsterfullerene molecule has been characterized by theoretical means.[18] A more general class of Stone−Wales-type reactions, in which a C_2 bond rotates 90° irrespective of the number of atoms in the surrounding polygons, has also been studied.[19] Both Stone−Wales studies employed the semiempirical MNDO method, as well as HF and DFT methods.

Results from these studies predict that the barrier to Stone−Wales-type rearrangements is, in general, ~6−7 eV, which is the highest barrier of any reaction in the present fullerene assembly model. However, by the time cage closure occurs, an enormous lowering of the electronic energy of the cluster has taken place, with a corresponding conversion of that energy to vibration. This vibrational energy is the means whereby the annealing barriers can be overcome. To illustrate the magnitude of the lowering of the electronic energy, DZP BP calculations have been performed on several fullerenes, with comparison to the energies of the original monocyclic rings, and the results are shown in Table 10. Since fullerenes are more stable than monocyclic rings by 20 eV and more, overcoming the barriers to annealing is not a problem. Therefore, cages that form from the hoops are able to isomerize to find the most stable structure. TB energetics for a complete path from rings to the most stable
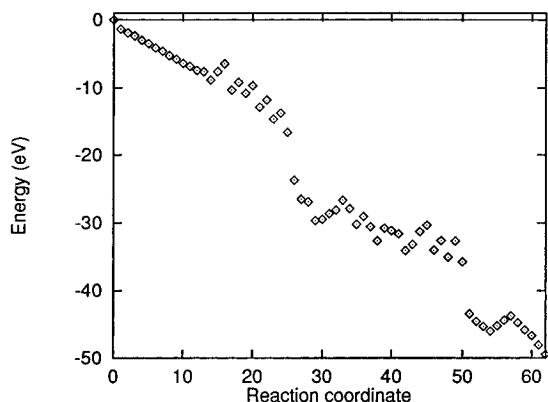
Figure 11. TB energetics for a path from two C_{30} rings to C_{60} buckminsterfullerene (minima only, represented by diamonds).
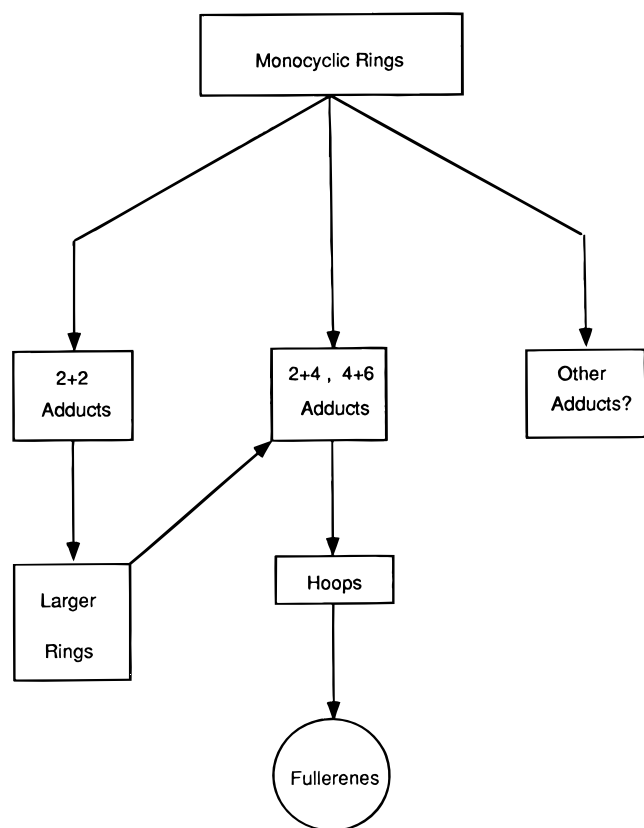

Figure 12. The cycloaddition model for fullerene formation.

fullerene are shown for C_{36} and C_{60} in Figures 10 and 11, respectively.

Conclusion

The cycloaddition model is consistent with current experimental results and elucidates the road to fullerenes with energetic information obtained at high levels of theory. Also, this model is simply a path to closure of a carbon cage, any cage, rather than relying on contrived mechanisms which are directed toward specific cages. Annealing and fragmentation are all that is required to bring buckminsterfullerene to prominence. These are the advantages of the model.

In the cycloaddition model, experimentally observed monocyclic rings collide to create a variety of cycloadducts. The appearance of $2 + 2$, $2 + 4$, and $4 + 6$ cycloadducts can be supported by experimental data. The $2 + 2$ adducts open via a retro-$2 + 2$ process to form larger monocyclic rings, which could be called "second-generation" rings. Second-generation rings collide with other rings to form large cycloadducts. Large $2 + 2$ cycloadducts can open to form third-generation rings, and so on. The $2 + 4$ and $4 + 6$ cycloadducts do not have a low-energy path to second-generation monocyclic rings. Rather, they undergo a series of cyclizations to form carbon hoops. Carbon hoops undergo 1,2-carbon shifts and further cyclizations to generate closed cages. These cages anneal to find the most stable isomer. The elements of the cycloaddition model are represented graphically in Figure 12.

The cycloaddition model is a useful tool for understanding fullerene formation. This model is a synthesis of experimental observations and theoretical predictions. A new interpretation of the graphite vaporization ion chromatography results is developed into a fullerene assembly model based on reactions which are shown by theoretical calculations to have reasonable energetics. We believe that this cycloaddition model is a novel, successful approach toward the understanding of the fullerene formation process.

References and Notes

(1) Kroto, H. W.; Heath, J. R.; O'Brien, S. C.; Curl, R. F.; Smalley, R. E. *Nature* **1985**, *318*, 162.
(2) Krätschmer, W.; Lamb, L. D.; Fostiropoulos, K.; Huffman, D. R. *Nature* **1990**, *347*, 354.
(3) Ebbesen, T. W.; Tabuchi, J.; Tanigaki, K. *Chem. Phys. Lett.* **1992**, *191*, 336.
(4) McElvany, S. W.; Ross, M. M.; Goroff, N. S.; Diederich, F. *Science* **1993**, *259*, 1594.
(5) Kemper, P. R.; Bowers, M. T. *J. Am. Soc. Mass Spectrom.* **1990**, *1*, 197. Kemper, P. R.; Bowers, M. T. *J. Phys. Chem.* **1991**, *95*, 5134.
(6) von Helden, G.; Hsu, M.-T.; Gotts, N.; Bowers, M. T. *J. Phys. Chem.* **1993**, *97*, 8182.
(7) Book, L. D.; Xu, C. H.; Scuseria, G. E. *Chem. Phys. Lett.* **1994**, *222*, 281.
(8) Strout, D. L.; Book, L. D.; Millam, J. M.; Xu, C. H.; Scuseria, G. E. *J. Phys. Chem.* **1994**, *98*, 8622.
(9) Xu, C. H.; Wang, C. Z.; Chan, C. T.; Ho, K. M. *J. Phys. Condens. Matter* **1992**, *4*, 6047.
(10) Huzinaga, S. *J. Chem. Phys.* **1965**, *42*, 1293. Dunning, T. H., Jr. *J. Chem. Phys.* **1970**, *53*, 2823.
(11) Becke, A. D. *Phys. Rev. A* **1988**, *38*, 3098.
(12) Perdew, J. P.; Wang, Y. *Phys. Rev. B* **1992**, *45*, 13244. Perdew, J. P.; Chevary, J. A.; Vosko, S. H.; Jackson, K. A.; Singh, D. J.; Fiolhais, C. *Phys. Rev. B* **1992**, *46*, 6671.
(13) Ahlrichs, R.; Bär, M.; Häser, M.; Horn, H.; Kölmel, C. *Chem. Phys. Lett.* **1989**, *162*, 165.
(14) Odom, G. K.; Scuseria, G. E. Unpublished results.
(15) Hunter, J. M.; Fye, J. L.; Roskamp, E. J.; Jarrold, M. F. *J. Phys. Chem.* **1994**, *98*, 1810.
(16) Taylor, P. R.; Bylaska, E.; Weare, J. H.; Kawai, R. *Chem. Phys. Lett.* **1995**, *235*, 558.
(17) Stone, A. J.; Wales, D. J. *Chem. Phys. Lett.* **1986**, *128*, 501.
(18) Murry, R. L.; Strout, D. L.; Odom, G. K.; Scuseria, G. E. *Nature* **1993**, *366*, 665.
(19) Murry, R. L.; Strout, D. L.; Scuseria, G. E. *Int. J. Mass Spectrom. Ion Proc.* **1994**, *138*, 113.